

Multiscale Analysis of the Performance of Micro/nano Porous Filtration Membranes with Double Concentric Cylindrical Pores: Part I-Analysis Development

Zhipeng TANG*, Yongbin ZHANG**

*College of Mechanical Engineering, Changzhou Vocational Institute of Mechatronic Technology, Changzhou, Jiangsu Province, China, E-mail: tzp2192@czimt.edu.cn

**College of Mechanical Engineering, Changzhou University, Changzhou, Jiangsu Province, China
E-mail: yongbinzhang@cczu.edu.cn; engmech1@sina.com (Corresponding Author)

crossref <http://dx.doi.org/10.5755/j02.mech.30507>

1. Introduction

Nanoporous filtration membranes have been rapidly developed because of their important applications in water filtration, hemofiltration, DNA analysis, biosensors and drug delivery etc. [1–13]. Their advantages are the tiny filtration pores the radii of which are on the 1 nm or 10 nm scales. These filtration pores are sufficient for filtering out any particles, bacteria, virus and organic macro molecules. The studies on these membranes are mainly experimental [1–13], as the theoretical research on them is relatively more difficult. In recent years, Zhang used the developed flow equation for nanoscale flow to study the performances of different types of nanoporous filtration membranes [14].

In practice, there are such nanoporous filtration membranes in which the radii of the filtration pores are on the scales of 10 nm, 100 nm or even bigger. When the liquids flow through the filtration pores of these membranes, a molecular scale layer physically adsorbed to the pore wall will form, it will have an important influence on the flow inside the pore, while in the central region of the pore indeed occurs the continuum liquid flow. This is the multiscale flow occurring inside the nanoporous filtration membranes, which actually have been little addressed in the research. Although experiments may have been carried out a lot on these membranes with particular flow regimes, theoretical studies on them are more difficult, and the understandings on the performances of these membranes currently seem still scarce.

Recently, Zhang presented the theoretical derivation results for the multiscale flow in micro/nano cylindrical pores where the adsorbed layer effect plays, by ignoring the interfacial slippage on any interface [15].

Conventionally, a nanoporous filtration membrane consists of the very thin filtration layer containing dense nanoscale filtration pores and the supporting layer containing much bigger micro pores [12, 13]. The micro pores in the supporting layer is for increasing the flux, but their radii and distributions on the membrane surface are normally not optimized.

The present paper presents a theoretical study on the performance of the nanoporous filtration membrane where the above mentioned multiscale flow occurs. Across the membrane thickness is distributed in sequence two concentric cylindrical pores with different radii; The small nano pore is for filtration, while the bigger micro/nano

pore is for reducing the flow resistance and increasing the flux of the membrane. Although the filtration membrane with such a geometrical design has been addressed by Zhang, he studied this kind of membrane by assuming the liquid flow in the filtration pore as completely non-continuum across the pore radius [14]. His analysis is valid when the radius of the filtration pore is sufficiently small so that all the liquid becomes non-continuum across the pore radius. However, the radius of the filtration pore in the present membrane may be much bigger so that the multiscale flow occurs inside the filtration pore; Inside the other bigger pore, which is for reducing the flow resistance, may also occur the multiscale flow. For the present membrane, the theoretical analysis is radically different from the previous ones, and the obtained results may also be fresh and of particular interest to the engineering design.

2. The configuration of the studied membrane

Fig. 1, a shows the studied micro/nano porous filtration membrane where the radii of the pores are not so small that near the pore wall occurs the flow of the adjacent layers (i.e. the adsorbed layer flow) and in the central region of the pore occurs the continuum liquid flow as shown in Fig. 1, b. The flow regime in this membrane has been recognized and is actually multiscale [16]; it governs the flux of the membrane. The present membrane may be used to filter out impurities such as tiny particles, bacteria, virus or organic macro molecules, however the total flow rate through the membrane may consist of both the adsorbed layer flow and the continuum liquid flow because of the pore size. The surfaces of all the pore walls are identical. The pore with the radius R_0 is for filtration, and its axial length is l_0 . The pore with the radius R_1 is bigger ($R_1 > R_0$) and for reducing the flow resistance and increasing the flux of the membrane, and its axial length is l_1 . The thickness of the membrane is l . The configuration of the present membrane is the same with that of the membrane studied before by Zhang, except that the radii of the pores in the present membrane are larger or even much larger than those in Zhang's earlier membrane [14]. Although Zhang has given the optimization results for the optimum value of R_1 / R_0 for the highest flux of the membrane based on the non-continuum flow assumption inside the filtration pore in the condition of very small radii of the

filtration pore [14], it is obvious that the new analysis should be developed for the present membrane, the design optimization of which should be based on the corresponding multiscale flow theory.

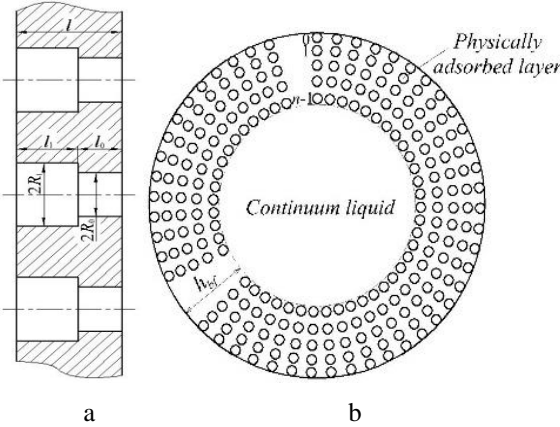


Fig. 1 The studied nanoporous filtration membrane with multiscale flow: a) the membrane profile; b) flowing media inside the magnified filtration pore

3.1. Mass flow rate through the pore

The mass flow rate through the filtration pore in the present membrane is [15]:

$$q_{m,b} = 2\pi R_{e,0} \left[\frac{h_{bf}^3}{2\eta_{bf}^{eff}} \frac{\Delta p_0}{l_0} \left(1 + \frac{1}{2\lambda_{bf,0}} - \frac{q_0 - q_0^n}{q_0^{n-1} - q_0^n} \frac{\Delta_{n-2}}{h_{bf}} \right) \frac{\varepsilon}{1 + \frac{\Delta x}{D}} - \frac{F_1 h_{bf}^3}{12\eta_{bf}^{eff}} \frac{\Delta p_0}{l_0} \rho_{bf}^{eff} + \right. \\ \left. + \left\{ \frac{1}{4\eta} - \frac{4}{\eta_{bf}^{eff}} \left[\frac{F_2 \lambda_{bf,0}^2}{6} - \frac{\lambda_{bf,0}}{1 + \frac{\Delta x}{D}} \left(\frac{1}{2} + \lambda_{bf,0} - \frac{(q_0 - q_0^n) \Delta_{n-2}}{2(q_0^{n-1} - q_0^n)(R_0 - h_{bf})} \right) \right] \right\} \frac{\pi \Delta p_0 (R_0 - h_{bf})^4 \rho}{l_0} \right], \quad (1)$$

where: \$h_{bf}\$ is the thickness of the adsorbed layer; \$D\$ is the diameter of the liquid molecule; \$\Delta p_0\$ is the pressure drop on the filtration pore; \$R_{e,0} = R_0(1 - \lambda_x/2)\$, \$\lambda_{bf,0} = \lambda_x/[2(1 - \lambda_x)]\$, \$\lambda_x = h_{bf}/R_0\$, \$\rho\$ and \$\eta\$ are respectively the bulk density and the bulk viscosity of the liquid flowing through the membrane; \$\rho_{bf}^{eff}\$ and \$\eta_{bf}^{eff}\$ are respectively the average density and the effective viscosity of the adsorbed layer across the layer thickness; \$\eta_{bf}^{eff} = Dh_{bf}/[(n-1)(D + \Delta_x)(\Delta_l/\eta_{line,l})_{avr,n-1}]\$, \$q_0 = \Delta_{j+1}/\Delta_j\$ and \$q_0\$ is constant; \$\Delta x\$ is the separation between the neighboring liquid molecules in the flow direction in the adsorbed layer, \$\varepsilon = (2DI + II)/[h_{bf}(n-1)(\Delta_l/\eta_{line,l})_{avr,n-1}]\$, \$F_1 = \eta_{bf}^{eff}(12D^2\psi + 6D\varphi)/h_{bf}^3\$, \$F_2 = 6\eta_{bf}^{eff}D(n-1)(l\Delta_{l-1}/\eta_{line,l-1})_{avr,n-1}/h_{bf}^2\$, here:

$$q_{m,b} = 2\pi R_{e,1} \left[\frac{h_{bf}^3}{2\eta_{bf}^{eff}} \frac{\Delta p_1}{l_1} \left(1 + \frac{1}{2\lambda_{bf,1}} - \frac{q_0 - q_0^n}{q_0^{n-1} - q_0^n} \frac{\Delta_{n-2}}{h_{bf}} \right) \frac{\varepsilon}{1 + \frac{\Delta x}{D}} - \frac{F_1 h_{bf}^3}{12\eta_{bf}^{eff}} \frac{\Delta p_1}{l_1} \rho_{bf}^{eff} + \right. \\ \left. + \left\{ \frac{1}{4\eta} - \frac{4}{\eta_{bf}^{eff}} \left[\frac{F_2 \lambda_{bf,1}^2}{6} - \frac{\lambda_{bf,1}}{1 + \frac{\Delta x}{D}} \left(\frac{1}{2} + \lambda_{bf,1} - \frac{(q_0 - q_0^n) \Delta_{n-2}}{2(q_0^{n-1} - q_0^n)(R_1 - h_{bf})} \right) \right] \right\} \frac{\pi \Delta p_1 (R_1 - h_{bf})^4 \rho}{l_1} \right], \quad (2)$$

3. The multiscale flow analysis for the studied membrane

When the pore wall is hydrophobic, the wall slippage may occur in the pore and it can greatly increase the flux of the membrane [17–19]. When the pore wall is hydrophilic with the nanoscale pore radius, the wall slippage can also occur in the pore [20]. The wall slippage in the membrane is determined by the power loss on the membrane. In the case of the wall slippage, both the flow resistance and flux of the membrane are intimately related to the power loss on the membrane; Greater the power loss on the membrane, smaller the flow resistance of the membrane, and higher the flux of the membrane. In the condition of the wall slippage, the optimization of the geometrical parameter values of the present membrane should be dependent on the power loss on the membrane. As a first work, the present study assumes no interfacial slippage on any interface and derives the corresponding optimization analysis results. The obtained results can be further examined to be applicable or not for the case of the wall slippage.

$I = \sum_{i=1}^{n-1} i(\Delta_l/\eta_{line,l})_{avr,i}$, $II = \sum_{i=0}^{n-2} [i(\Delta_l/\eta_{line,l})_{avr,i} + (i+1)(\Delta_l/\eta_{line,l})_{avr,i+1}] \Delta_i$, $\psi = \sum_{i=1}^{n-1} i(l\Delta_{l-1}/\eta_{line,l-1})_{avr,i}$, $\varphi = \sum_{i=0}^{n-2} [i(l\Delta_{l-1}/\eta_{line,l-1})_{avr,i} + (i+1)(l\Delta_{l-1}/\eta_{line,l-1})_{avr,i+1}] \Delta_i$, $\eta_{line,j-1}$ and Δ_{j-1} are respectively the local viscosity and the separation between the j^{th} and $(j-1)^{th}$ molecules across the adsorbed layer thickness, and j and $(j-1)$ are respectively the order numbers of the molecules across the adsorbed layer thickness shown in Fig.1, b.

The mass flow rate through the flow resistance-reducing pore (with the radius R_1) in the present membrane is equated as [15]:

where: $\lambda_{bf,1} = h_{bf} / [2(R_1 - h_{bf})]$; $R_{e,1} = R_1 - h_{bf} / 2$ and Δp_1 is the pressure drop on the pore with the radius R_1 .

3.2. Flow resistance

The flow resistances of the single pores with the radii R_1 and R_0 in the present membrane are respectively [14]:

$$\begin{aligned} FUNC(R_0, l_0) &= 2\pi R_{e,0} \left[\frac{h_{bf}^3}{2l_0 \eta_{bf}^{eff}} \left(1 + \frac{1}{2\lambda_{bf,0}} - \frac{q_0 - q_0^n}{q_0^{n-1} - q_0^n} \frac{\Delta_{n-2}}{h_{bf}} \right) \frac{\varepsilon}{1 + \frac{\Delta x}{D}} - \frac{F_1 h_{bf}^3}{12l_0 \eta_{bf}^{eff}} \right] \rho_{bf}^{eff} + \\ &+ \left\{ \frac{1}{4\eta} - \frac{4}{\eta_{bf}^{eff}} \left[\frac{F_2 \lambda_{bf,0}^2}{6} - \frac{\lambda_{bf,0}}{1 + \frac{\Delta x}{D}} \left(\frac{1}{2} + \lambda_{bf,0} - \frac{(q_0 - q_0^n) \Delta_{n-2}}{2(q_0^{n-1} - q_0^n)(R_0 - h_{bf})} \right) \right] \right\} \frac{\pi (R_0 - h_{bf})^4 \rho}{l_0}, \end{aligned} \quad (4)$$

$$\begin{aligned} FUNC(R_1, l_1) &= 2\pi R_{e,1} \left[\frac{h_{bf}^3}{2l_1 \eta_{bf}^{eff}} \left(1 + \frac{1}{2\lambda_{bf,1}} - \frac{q_0 - q_0^n}{q_0^{n-1} - q_0^n} \frac{\Delta_{n-2}}{h_{bf}} \right) \frac{\varepsilon}{1 + \frac{\Delta x}{D}} - \frac{F_1 h_{bf}^3}{12l_1 \eta_{bf}^{eff}} \right] \rho_{bf}^{eff} + \\ &+ \left\{ \frac{1}{4\eta} - \frac{4}{\eta_{bf}^{eff}} \left[\frac{F_2 \lambda_{bf,1}^2}{6} - \frac{\lambda_{bf,1}}{1 + \frac{\Delta x}{D}} \left(\frac{1}{2} + \lambda_{bf,1} - \frac{(q_0 - q_0^n) \Delta_{n-2}}{2(q_0^{n-1} - q_0^n)(R_1 - h_{bf})} \right) \right] \right\} \frac{\pi (R_1 - h_{bf})^4 \rho}{l_1}. \end{aligned} \quad (5)$$

The flow resistance of the whole membrane is [14]:

$$i_f = \frac{\Delta p}{q_m} = \frac{\Delta p_0 + \Delta p_1}{N q_{m,b}} = \frac{i_{f,0} + i_{f,1}}{N}, \quad (6)$$

where: Δp is the pressure drop on the membrane; q_m is the mass flow rate through the whole membrane; N is the number of the pores with the radius R_1 on the membrane surface; here $N = \lambda_N A_m$ where λ_N is the number density of the pore with the radius R_1 on the membrane surface and A_m is the area of the membrane surface.

If the production rate of the pore with the radius R_1 on the membrane surface is χ , $\chi = \pi \lambda_N R_1^2$ [14]. Then,

$1/N = \pi R_1^2 / (\chi A_m)$. Eq. (6) becomes:

$$\begin{aligned} FUNC(R_0, l_0) &= \frac{4\eta l FUNC(R_0, l_0)}{\pi \rho R_1^2 R_r^2} = \\ &= \left\{ \frac{4R_{e,0} \lambda_x^3}{C_y R_0 \lambda_0} \left[\left(1 + \frac{1}{2\lambda_{bf,0}} - \frac{q_0 - q_0^n}{q_0^{n-1} - q_0^n} \frac{\Delta_{n-2}}{h_{bf}} \right) \frac{\varepsilon}{1 + \frac{\Delta x}{D}} - \frac{F_1}{6} \right] C_q + \right. \\ &\left. + \frac{(1 - \lambda_x)^4}{\lambda_0} \left\{ 1 - \frac{8}{C_y} \left[\frac{F_2 \lambda_{bf,0}^2}{3} - \frac{2\lambda_{bf,0}}{1 + \frac{\Delta x}{D}} \left(\frac{1}{2} + \lambda_{bf,0} - \frac{(q_0 - q_0^n) \Delta_{n-2}}{2(q_0^{n-1} - q_0^n)(R_0 - h_{bf})} \right) \right] \right\} \left(\frac{R_0}{R_1} \right)^2 \left(\frac{R_0}{R_r} \right)^2 \right\}, \end{aligned} \quad (9)$$

$$\begin{aligned} i_{f,1} &= \frac{\Delta p_1}{q_{m,b}} = \frac{1}{FUNC(R_1, l_1)}, \\ i_{f,0} &= \frac{\Delta p_0}{q_{m,b}} = \frac{1}{FUNC(R_0, l_0)}. \end{aligned} \quad (3)$$

According to Eqs. (1) and (2), it is formulated that:

According to Eqs. (1) and (2), it is formulated that:

According to Eqs. (1) and (2), it is formulated that:

$$i_f = \left[\frac{1}{FUNC(R_0, l_0)} + \frac{1}{FUNC(R_1, l_1)} \right] \frac{\pi R_1^2}{\chi A_m}. \quad (7)$$

The dimensionless flow resistance of the membrane is defined as: $I_f = i_f \rho \chi A_m R_r^2 / (4\eta l)$, where R_r is a constant reference radius [14]. The dimensionless flow resistance of the present membrane is:

$$I_f = \frac{1}{FUNC(R_0, l_0)} + \frac{1}{FUNC(R_1, l_1)} = F \cdot \left(\frac{R_r}{R_0} \right)^2, \quad (8)$$

where:

$$\begin{aligned}
FUNC(R_1, l_1) &= \frac{4\eta l FUNC(R_1, l_1)}{\pi \rho R_1^2 R_r^2} = \\
&= \left\{ \frac{4R_{e,1}\lambda_x^3}{C_y R_0(1-\lambda_0)} \left[\left(1 + \frac{1}{2\lambda_{bf,1}} - \frac{q_0 - q_0^n}{q_0^{n-1} - q_0^n} \frac{\Delta_{n-2}}{h_{bf}} \right) \frac{\varepsilon}{1 + \frac{\Delta x}{D}} - \frac{F_1}{6} \right] C_q + \right. \\
&\quad \left. + \frac{\left(\frac{R_1}{R_0} - \lambda_x \right)^4}{1 - \lambda_0} \left\{ 1 - \frac{8}{C_y} \left[\frac{F_2 \lambda_{bf,1}^2}{3} - \frac{2\lambda_{bf,1}}{1 + \frac{\Delta x}{D}} \left(\frac{1}{2} + \lambda_{bf,1} - \frac{(q_0 - q_0^n)\Delta_{n-2}}{2(q_0^{n-1} - q_0^n)(R_1 - h_{bf})} \right) \right] \right\} \left(\frac{R_0}{R_1} \right)^2 \left(\frac{R_0}{R_r} \right)^2 \right\}, \quad (10)
\end{aligned}$$

here: $\lambda_0 = l_0 / l$, $C_y = \eta_{bf}^{eff} / \eta$, and $C_q = \rho_{bf}^{eff} / \rho$. Eq. (8) shows that for given values of R_r and R_0 , the function F can measure the dimensionless flow resistance of the present membrane.

4. Calculation

Exemplary calculations were made for a weak liquid-pore wall interaction. In these calculations, it was taken that $\Delta x / D = \Delta_{n-2} / D = 0.15$ and $\eta_{line,i} / \eta_{line,i+1} = q_0^m$, where q_0 and m are respectively positive constant [14, 15].

The parameter C_y is formulated as [14, 15]:

$$\varepsilon = 4.56 \times 10^{-6} (\Delta_{n-2} / D + 31.419)(n + 133.8)(q_0 + 0.188)(m + 41.62), \quad (13)$$

$$F_1 = 0.18(\Delta_{n-2} / D - 1.905)(\ln n - 7.897), \quad (14)$$

$$F_2 = -3.707 \times 10^{-4} (\Delta_{n-2} / D - 1.99)(n + 64)(q_0 + 0.19)(m + 42.43). \quad (15)$$

The values of other parameters were taken as: $m = 0.5$; $n = 3$; $q_0 = 1.03$; $h_{cr,bf} = 7$ nm.

According to the above input parameter values, the thickness of the adsorbed layer was calculated to be $h_{bf} = 1.32$ nm.

5. Results

Figs. 2, a-c respectively show the calculated dimensionless flow resistances of the studied membrane for the weak liquid-pore wall interaction when $\lambda_x = 0.5$, 0.2 and 0.1. All the calculated results show that there is the optimum value of the ratio R_1/R_0 which gives the lowest flow resistance and thus the highest flux of the membrane. This optimum R_1/R_0 value normally ranges between 1.0 and 2.0. The figures indicate that the increase of R_1/R_0 will increase the flow resistance of the membrane and thus reduce the flux of the membrane when R_1/R_0 is greater than the optimum one, particularly for high R_1/R_0 values. These show that an over large value of R_1 is indeed not beneficial for the flux of the membrane. For given values of λ_x and R_1/R_0 , the flow resistance of the membrane is significantly increased with the increase of λ_0 , particularly for large values of R_1/R_0 . It shows that the increase of the axial length l_0 of the filtration pore has a significantly negative effect on the flux of the membrane and the value of l_0 should be as small as possible. Figs. 2, a-c all show that for the present membrane, the ratio of R_1/R_0 should be designed as the optimum value, not only because of the

$$C_y(H_{bf}) = 0.9507 + \frac{0.0492}{H_{bf}} + \frac{1.6447E-4}{H_{bf}^2}, \quad (11)$$

where: $H_{bf} = h_{bf} / h_{cr,bf}$ and $h_{cr,bf}$ is a critical thickness.

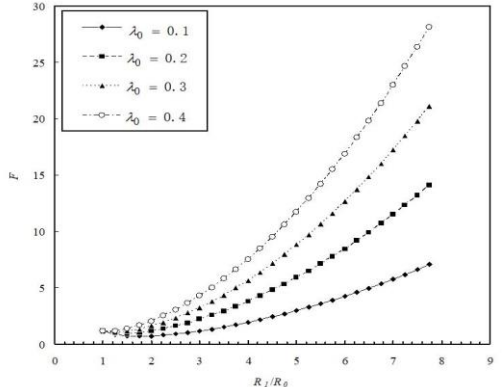
The parameter C_q is formulated as [14, 15]:

$$C_q = 1.116 - 0.328H_{bf} + 0.253H_{bf}^2 - 0.041H_{bf}^3. \quad (12)$$

The parameters ε , F_1 and F_2 are respectively formulated as [15]:



a) $\lambda_x = 0.5$



b) $\lambda_x = 0.2$

Fig. 2 Calculated dimensionless flow resistances of the studied membrane for the weak liquid-pore wall interaction

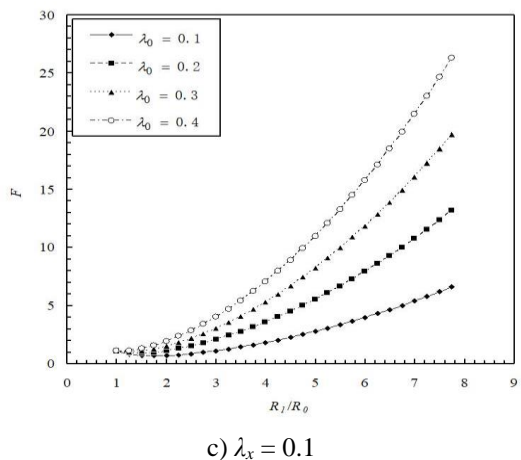


Fig. 2 Continuation

resulting highest flux of the membrane but also because of the smallest influences of the variations of both the values of the parameters l_0 and R_1 on the flow resistance and thus the flux of the membrane. The present membrane should have the best performance when the value of R_1/R_0 is optimum, not only from the viewpoint of the flux but also from the viewpoint of the membrane manufacturing, allowing the tolerable variations of both l_0 and R_1 .

6. Conclusions

A multiscale analysis is presented for the flux and flow resistance of micro/nano porous filtration membranes where multiscale flows occur. Principally, when a liquid flows through these membranes, there is a layer formed on and physically adsorbed to the pore wall surface. When the radius of the filtration pore is in such a range that the thickness of the adsorbed layer is on the same scale with the radius of the filtration pore, the adsorbed layer flow is comparable with the continuum liquid flow in the central region of the pore, and the multiscale analysis is required for calculating the flux of the membranes by incorporating both the adsorbed layer flow and the continuum liquid flow.

The present study uses the flow factor approach model for nanoscale flow to simulate the adsorbed layer flow and uses the Newtonian fluid model to simulate the continuum liquid flow. The equations are respectively given for the mass flow rates of these two flows. The flow resistances of the pores and the membrane are defined.

The analysis was particularly carried out for micro/nano porous filtration membranes with double concentric cylindrical pores, where across the membrane thickness are distributed in sequence two cylindrical pores with different radii, the smaller pore with the radius R_0 is for filtration and the larger pore with the radius R_1 is for reducing the flow resistance. The dimensionless flow resistance of this membrane was formulated by the closed-form explicit equation based on the derived multiscale flow equations. Exemplary calculations were made for a weak liquid-pore wall interaction.

The multiscale calculation results show that there is the optimum value of the ratio R_1/R_0 for the lowest flow resistance and thus the highest flux of the membrane. The increase of R_1 is not beneficial for the flux of the membrane when R_1/R_0 is over the optimum value. An over large

R_1 will result in the sensitive variation of the flow resistance of the membrane with the variations of both R_1 and the axial length l_0 of the filtration pore. From the engineering viewpoint, the ratio R_1/R_0 should be designed as the optimum value, allowing the tolerable variations of both l_0 and R_1 .

References

1. Ariono, D.; Aryanti, P. T. P.; Wardani, A. K.; Wenthen, I. G. 2018. Fouling characteristics of humic substances on tight polysulfone-based ultrafiltration membrane, *Membrane and Water Treatment* 9: 353-361. <https://doi.org/10.12989/mwt.2018.9.5.353>.
2. Baker, L. A.; Bird, S. P. 2008. Nanopores: A makeover for membranes, *Nature Nanotechnology* 3: 73-74. <http://dx.doi.org/10.1038/nnano.2008.13>.
3. El-ghizel, S.; Jalté, H.; Zeggar, H.; Zait, M.; Belhamidi, S.; Tiyal, F.; Hafsi, M.; Taky, M.; Elmidouai, A. 2019. Autopsy of nanofiltration membrane of a decentralized demineralization plant, *Membrane and Water Treatment* 10: 277-286. <https://doi.org/10.12989/mwt.2019.10.4.277>.
4. Fissel, W. H.; Dubnisheva, A.; Eldridge, A. N.; Fleischman, A. J.; Zydny, A. L.; Roy, S. 2009. High-performance silicon nanopore hemofiltration membranes, *Journal of Membrane Science* 326: 58-63. <http://dx.doi.org/10.1016/j.memsci.2008.09.039>.
5. Jackson, E. A.; Hillmyer, M. A. 2010. Nanoporous membranes derived from block copolymers: From drug delivery to water filtration, *ACS Nano* 4: 3548-3553. <http://dx.doi.org/10.1021/nn1014006>.
6. Jin, Y.; Choi, Y.; Song, K. G.; Kim, S.; Park, C. 2019. Iron and manganese removal in direct anoxic nanofiltration for indirect potable reuse, *Membrane and Water Treatment* 10: 299-305. <https://doi.org/10.12989/mwt.2019.10.4.299>.
7. Jung J.; Shin B.; Park K. Y.; Won S.; Cho J. 2019. Pilot scale membrane separation of plating wastewater by nanofiltration and reverse osmosis, *Membrane and Water Treatment* 10: 239-244. <https://doi.org/10.12989/mwt.2019.10.3.239>.
8. Li, N.; Yu, S.; Harrell, C.; Martin, C. R. 2004. Conical nanopore membranes: Preparation and transport properties, *Analytical Chemistry* 76: 2025-2030. <http://dx.doi.org/10.1021/ac035402e>.
9. Rashidi, H.; Meriam, N.; Sulaiman, N.; Hashim, N. A.; Bradford, L.; Asgharnejad, H.; Larijani, M. 2020. Development of the ultra/nano filtration system for textile industry wastewater treatment, *Membrane and Water Treatment* 11: 333-344. <https://doi.org/10.12989/mwt.2020.11.5.333>.
10. Surwade, S. P.; Smirnov, S. N.; Vlassiouk, I. V.; Unocic, R. R.; Veith, G. M.; Dai, S.; Mahurin, S. M. 2015. Water desalination using nanoporous single-layer grapheme, *Nature Nanotechnology* 10: 459-464. <https://doi.org/10.1038/nnano.2015.37>.
11. Tiraferrri, A.; Yip, N. Y.; Phillip, W. A.; Schiffman, J. D.; Elimelech, M. 2011. Relating performance of thin-film composite forward osmosis membranes to support layer formation and structure, *Journal of Membrane Science* 367: 340-352.

- http://dx.doi.org/10.1016/j.memsci.2010.11.014.
12. **Yang, S. Y.; Ryu, I.; Kim, H. Y.; Kim, J. K.; Jang, S. K.; Russell, T. P.** 2006. Nanoporous membranes with ultrahigh selectivity and flux for the filtration of viruses, *Advanced Materials* 18: 709-712.
<https://doi.org/10.1002/adma.200501500>.
13. **Yip, N. Y.; Tiraferri, A.; Phillip, W. A.; Schiffman, J. D.; Elimelech, M.** 2010. High performance thin-film composite forward osmosis membrane, *Environmental Science Technology* 44: 3812-3818.
<http://dx.doi.org/0.1021/es1002555>.
14. **Zhang, Y. B.** 2018. Optimum design for cylindrical-shaped nanoporous filtration membrane, *International Communications in Heat and Mass Transfer* 96: 130-138.
<https://doi.org/10.1016/j.icheatmasstransfer.2018.06.003>.
15. **Zhang, Y. B.** 2020. Modeling of flow in a micro cylindrical tube with the adsorbed layer effect: Part I-Results for no interfacial slippage, *International Journal of Heat and Mass Transfer*: submitted.
16. **Atkas, O.; Aluru, N. R.** 2002. A combined continuum/DSMC technique for multiscale analysis of microfluidic filters, *Journal of Computational Physics* 178: 342-372.
17. **Liu, C.; Li, Z.** 2011. On the validity of the Navier-Stokes equations for nanoscale liquid flows: The role of channel size, *AIP Advance* 1: 032108.
<https://doi.org/10.1063/1.3621858>.
18. **Ritos, K.; Mattia, D.; Calabro, F.; Reese, J. M.** 2014. Flow enhancement in nanotubes of different materials and lengths, *Journal of Chemical Physics* 140: 014702.
<https://doi.org/10.1063/1.4846300>.
19. **Mattia, D.; Calabro, F.** 2012. Explaining high flow rate of water in carbon nanotubes via solid-liquid molecular interactions, *Microfluidics and Nanofluidics* 13: 125-130.
<https://doi.org/10.1007/s10404-012-0949-z>.
20. **Koklu, A.; Li, J.; Sengor, S.; Beskok, A.** 2017. Pressure-driven water flow through hydrophilic alumina nanomembranes, *Microfluidics and Nanofluidics* 21: 24-135.
<https://doi.org/10.1007/s10404-017-1960-1>.

Z. Tang, Y. Zhang

MULTISCALE ANALYSIS OF THE PERFORMANCE OF MICRO/NANO POROUS FILTRATION MEMBRANES WITH DOUBLE CONCENTRIC CYLINDRICAL POLES: PART I-ANALYSIS DEVELOPMENT

S u m m a r y

In nanoporous filtration membranes, when the radius of the filtration pore is so big that the flow of the adsorbed layer on the pore wall is comparable with the flow of the continuum fluid in the central region of the pore, the multiscale analysis is required for estimating the performance of the membranes. The present paper presents such a multiscale analysis for the performance of nanoporous filtration membranes with double concentric cylindrical pores. The dimensionless flow resistance of the membrane was calculated for a weak fluid-pore wall interaction for varying operational parameter values. It was found that there is the optimum ratio of the radius of the filtration pore to the radius of the other bigger pore for the highest flux of the membrane.

Keywords: adsorbed layer, filtration, multiscale flow, membrane, nanopore.

Received January 21, 2022

Accepted June 14, 2022



This article is an Open Access article distributed under the terms and conditions of the Creative Commons Attribution 4.0 (CC BY 4.0) License (<http://creativecommons.org/licenses/by/4.0/>).